Korean J. Chem. Eng., 34(3), 757-767 (2017)
DOI: 10.1007/s11814-016-0330-0

pISSN: 0256-1115
eISSN: 1975-7220

Response surface modeling, isotherm, thermodynamic and optimization study of arsenic (V) removal from aqueous solutions using modified bentonite-chitosan (MBC)

Mohammad Hadi Dehghani*,, Ahmad Zarei*,†, Alireza Mesdaghinia*, Ramin Nabizadeh*, Mahmood Alimohammadi*, and Mojtaba Afsharnia*****

*Department of Environmental Health Engineering, School of Public Health, Tehran University of Medical Sciences, Tehran, Iran
**Institute for Environmental research, Center for Solid Waste Research, Tehran University of Medical Sciences, Tehran, Iran
***Department of Environmental Health Engineering, School of Public Health, Gonabad University of Medical Sciences, Gonabad, Iran
(*Received 6 September 2016 • accepted 20 November 2016*)

Abstract−Arsenic contamination, a worldwide concern, has received a great deal of attention due to its toxicity and carcinogenicity. In the present study, we focused on the combined application of modified bentonite and chitosan (MBC) for the removal of As(V). Arsenic removal experiments were carried out to determine the amount of As(V) adsorbed as a function of pH (2-8), sorbent dosage (0.1-1.5 g/L), As(V) concentration (20-200 mg/L) and time (60-240 min). The system was optimized by means of response surface methodology. The analysis of variance (ANOVA) of the quadratic model demonstrated that the model was highly significant (R^2≈97.3%). Optimized values of pH, sorbent dosage, initial As(V) concentration and time were found to be 3.7, 1.40 g/L, 69 mg/L, and 167 min, respectively. The results reveal that the prepared adsorbent has a high adsorption capacity (122.23 mg/g) for As(V) removal. Among the isotherm models used, the Langmuir isotherm model was the best fit for the obtained data. The adsorption kinetics following a pseudo-second-order kinetic model was involved in the adsorption process of As(V). Thermodynamic studies confirmed the spontaneous and endothermic character of adsorption process.

Keywords: Adsorption, Chitosan, As(V), Modified Bentonite, Response Surface Modeling

INTRODUCTION

Arsenic contamination as a worldwide concern, has received a great deal of attention due to its toxicity and carcinogenicity [1]. Arsenic contamination of water has been reported from the United States, China, Mexico, Germany, Bangladesh, Bolivia, Japan, India and Iran [2-4]. In natural water, arsenic is primarily present in two states: arsenite, As(III), and arsenate, As(V), [5]. High levels of arsenic in drinking water can cause a variety of adverse health effects, including dermal, cardiovascular, gastrointestinal, respiratory, mutagenic, genotoxic, and carcinogenic effects [6]. Due to the prevalent contamination of surface and groundwater to arsenic and its high toxicity to humans and other organisms, the USEPA and the WHO [7] have recently revised the maximum concentration level for arsenic in drinking water by decreasing it from 50 to 10 μg/L. A number of treatment techniques such as precipitation, coagulation, membrane separation, adsorption and ion-exchange have been developed and applied for arsenic removal, but each method has inherent limitations [8]. The utilization of bio-adsorbents, including chitin and chitosan composites for the treatment of waters and wastewaters containing heavy metal, is gaining more attention as simple, effective and economical means of contamination remediation [2]. Generally, chitosan results from the deacetylation of chitin with a strong basic solution [9], which is abundantly available as a major component of crustacean shells such as insects, prawns, crabs and shrimps in nature. Chitosan is the world's second most abundant natural biopolymer after cellulose [10]. This polymer contains amin (-NH_2) and hydroxyl (-OH) groups in its structure, which is useful for chemical modifications and can be efficiently used as a potential adsorbent in the removal of many contaminants including most metal ions and dyes from aqueous solutions. From the other side, chitosan becomes soluble in acidic environment, which might be a limiting step for its applicability. Therefore, chitosan can be cross-linked to render it insoluble in acidic media. Furthermore, to improve its adsorption capacity and resistance to low pH values, chitosan can be immobilized on other materials [11]. Based on Wan et al's study, immobilizing chitosan on a low-cost material would result in less quantity of chitosan being used without changing its metal adsorption capacity [12]. Recently, several studies focused in utilizing chitosan immobilized on bentonite and chitosan-coated bentonite for the removal of Ni(II), Pb(II) [13], Cu(II) [14], and oxidized sulfur compounds [15] from aqueous

†To whom correspondence should be addressed.
E-mail: a.zarei.tums@gmail.com

solution under static conditions. In the present study, the adsorption capability of chitosan was improved by the incorporation of bentonite. Bentonite, as a low-cost, widely distributed and abundant inorganic matter worldwide, is effective for the removal of toxic contaminants and has high adsorptive and ion exchange properties [16]. However, bentonite cannot efficiently remove As(V) anionic states from aqueous solution due to its negatively charged surface. Therefore, it can often be modified by a variety of physical and chemical methods to achieve the desired surface properties [17]. Several studies have reported cationic quaternary amine compounds or surfactants for the modification of clay minerals. In fact, modifications of bentonite with cationic quaternary amine compounds have attracted considerable attention because they provide bentonite with the potential to behave as anionic exchanger and change the surface properties from hydrophilic to hydrophobic [18]. Hence, our aim was to fabricate inorgano-organo sodium bentonites and investigate the adsorption of As(V) on the modified bentonite chitosan (MBC). The Ca-bentonite was modified by three procedures: Na_2CO_3 (BNa), thermal and compound treatment by CTAB. Na_2CO_3 enhances the rate of water adsorption and the expansion ratio of bentonite. Thermal treatment removes water from the surface or between the layers, and enhances the specific surface area of the bentonite. Compound modification by a surface active agent could make its water treatment effect stronger [19]. Many scientists have focused on chitosan as a promising adsorbent because of its biodegradability, non-toxicity, and chelating ability with metals [20]. To the best of our knowledge, the present treatment methodology has not yet been reported for the removal of As(V). Thus, we focused on the investigation of the application of naturally abundant and less expensive adsorbents such as chitosan and bentonite/chitosan biocomposite in the removal of As(V). The study also emphasizes the removal of As(V) at varying conditions of pH, sorbent dosage, contaminant concentration and contact time. The other objective was to evaluate adsorption capacity of the new sorbent for As(V) removal under equilibrium experimental conditions. In the present work, the experimental design and optimization of process parameters affecting As(V) removal was done by RSM under "R" software [21].

EXPERIMENTAL METHODS

1. Reagents and Instruments

All the chemicals used in the present work were of analytical grade. Chitosan with 90% degree of deacetylation and Ca-bentonite were purchased from Sigma-Aldrich. The cationic surfactant selected for this study was cetyl trimethylammonium bromide (CTAB) from Sigma-Aldrich. An atomic absorption spectrophotometer (AA1700, China) was employed for determination of residual concentrations of As(V). $Na_2HAsO_4{\cdot}7H_2O$, sodium carbonate, oxalic acid, sodium hydroxide, hydrochloric acid, nitric acid were also purchased from Sigma-Aldrich. All pH values were measured with a Sartorius PB-11 pH meter, Germany. Double distilled water was used throughout the experiments. As(V) working solutions were immediately prepared by diluting arsenic solutions with deionized water before use. The cation exchange capacity (CEC) of calcium bentonite was 132.31 meq/100 g. The chemical composition of Ca-bentonite as w% was in the following order: SiO_2 (61.1), Al_2O_3 (18.43), MgO (3.33), Fe_2O_3 (3.1), Na_2O (1.8), CaO (0.09). The real density of Ca-bentonite was 2.5121 ± 0.0032 g/cm^3.

2. Preparation of Modified Bentonite

The modified bentonite was prepared as proposed by Gao et al. [19], in which, briefly, Ca-bentonite was treated through three procedures: Na_2CO_3 treatment (BNa), thermal treatment and compound treatment by CTAB. Initially, for Na_2CO_3 treatment, 500 g of Ca-bentonite was added into a beaker containing ethanol solution (volume ratio=1 : 1). Na_2CO_3 in an amount of 4% of the Ca-bentonite was added into the slurry. The pH of the suspension was adjusted to 9.0 by adding 1 M NaOH. The slurry was agitated for 2 h in a shaker incubator at 80 °C with frequency 110 min^{-1} and centrifuged at 3,000 min^{-1} for 10 min. The solid residue was then washed several times with double distilled water until the absence of CO_3^{2-} was confirmed with $Ca(OH)_2$ test. The sample was dried overnight at 105 °C. For thermal treatment, the prepared BNa was placed in an oven at 450 °C for 2 h. Finally, for compound modification, 20 g of CTAB was prepared in a 1 L volumetric flask. The CTAB solution and 100 g of BNa were added to 1 L Erlenmeyer flask and agitated for 2 h at 30 °C. Afterward, the modified bentonite was filtered and washed several times with deionized water to eliminate bromide ions. The solid was dried at room temperature during 24 h, ground in a mortar, sieved and placed in a desiccator (Fig. 1).

3. Preparation of Modified Bentonite Chitosan (MBC)

Chitosan was coated onto bentonite according to Kalyani et al. [22]. Chitosan 90% (0.5 g) was slowly added into oxalic acid solution (volume fraction, 2%) under continuous stirring for 2 h, followed by addition of modified bentonite (25 g) prepared above over 12 h. The mixture was stirred for 6 h and later precipitated by NaOH

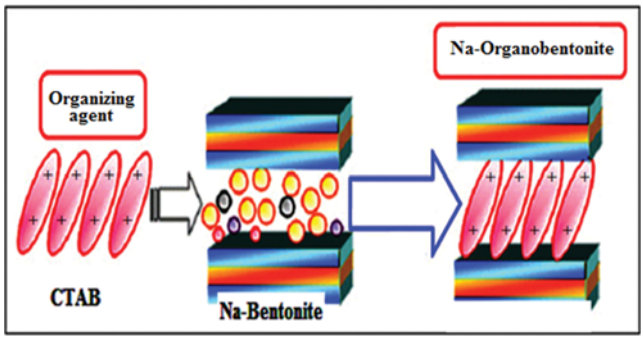

Fig. 1. CTAB modification of Na-bentonite treated thermally.

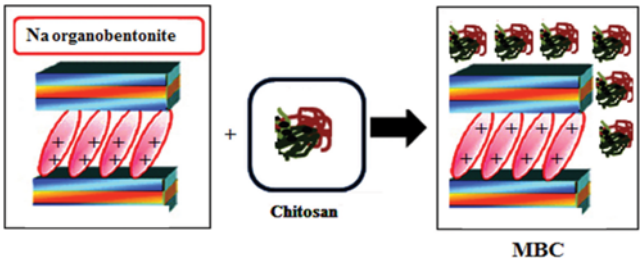

Fig. 2. Prepared modified bentonite chitosan (MBC).

(Fig. 2).

4. Adsorption Experiments

Batch adsorption experiments, designed by response surface methodology (RSM), were carried out at 25 °C and 150 rpm to investigate the effects of independent variables such as pH (2-8), sorbent dosage (0.1-1.5 g/L), initial concentrations of As(V) (20-200 mg/L), and contact time (60-240 min) on the removal of arsenic from aqueous environment by MBC. Different concentrations of test solutions were prepared by diluting the stock solution with suitable volume of distilled water. After the solution was shaken for a predetermined time, it was filtered through Whatman paper and the residual arsenic was analyzed to determine the removal efficiency of As(V) by atomic absorption spectroscopy (AAS). A desired amount of MBC was added to 1 liter of known concentration of As(V) ions in an incubator shaker at a constant speed of 150 rpm for various time intervals. The maximum adsorption capacity was obtained from the isotherm study. The equilibrium isotherms were fitted to the Freundlich, Langmuir and Temkin models. Finally, the removal efficiency (%) of As(V), and also the amount of arsenic adsorbed (Q_e, mg/g), were calculated using the following equations:

$$Q_e = \frac{(C_0 - C_e)V}{W} \quad (1)$$

$$\% \text{ Removal} = \frac{(C_0 - C_e) \times 100}{C_0} \quad (2)$$

where, C_0 and C_e are As(V) concentration in solution (mg/L) initially and at adsorption end, respectively, V is the volume of the solution (L), and W is the mass of the adsorbent (g).

5. Experimental Design and Procedure

The process variables affecting the removal of As(V) by MBC were studied using CCD central composite design in RSM using "R" software. The RSM was used to evaluate the combined effects of pH (X_1), MBC dosage (X_2), initial As(V) concentration (X_3) and contact time (X_4) on the adsorption process. The variable input parameters were a pH value in the range of 2.0-8.0, sorbent dosage of 0.1 to 1.5 g/L, initial As(V) concentration of 20-200 mg/L, and contact time in the range of 60-240 min, respectively. The factor levels were coded as −1 (low), 0 (medium) and 1 (high). A total of 44 runs were performed to optimize the process parameters and experiments were carried out according to the actual experimental design matrix.

The removal percentage of As(V) was chosen as the response of the system. The independent variables used in these experiments were coded according to the following equation:

$$A_i = \frac{X_i - X_0}{\Delta X} \quad (3)$$

Table 1. Experimental ranges and levels of the independent variables

Factors	Symbol	Range and levels (coded)		
		−1	0	1
pH	X_1	2	5	8
MBC dosage (g/L)	X_2	0.1	0.8	1.5
As(V) concentration (mg/L)	X_3	20	110	200
Time (min)	X_4	60	150	240

Table 2. Experimental design and results for the arsenic removal

Run order	X_1	X_2	X_3	X_4	Efficiency %	Run order	X_1	X_2	X_3	X_4	Efficiency %
1	3.5	0.45	65	195	44.7	23	5	0.8	110	150	52.8
2	6.5	0.45	65	195	23	24	5	0.8	110	150	53.8
3	5	0.8	110	150	55.9	25	2	0.8	110	150	47.8
4	3.5	0.45	155	105	25	26	5	0.8	200	150	42.5
5	5	0.8	110	150	55.5	27	5	0.8	20	150	67.4
6	5	0.8	110	150	52.7	28	5	0.1	110	150	17.6
7	5	0.8	110	150	50.7	29	5	0.8	110	150	58.4
8	3.5	1.15	155	105	44	30	5	0.8	110	240	59.5
9	6.5	1.15	155	195	49	31	5	0.8	155	150	51.9
10	6.5	0.45	155	195	24.4	32	6.5	0.45	65	105	18.5
11	5	0.8	110	150	53	33	6.5	1.15	155	105	16.5
12	5	0.8	110	150	53.1	34	5	0.8	110	150	59.5
13	3.5	0.45	155	195	33.7	35	3.5	1.15	155	195	75.4
14	3.5	1.15	65	105	60.9	36	5	0.8	110	150	53.8
15	6.5	1.15	65	195	64	37	3.5	1.15	65	195	93.7
16	6.5	1.15	65	105	44.1	38	3.5	0.45	65	105	32.6
17	5	0.8	110	150	47	39	8	0.8	110	150	12.5
18	6.5	0.45	155	105	10.6	40	5	0.8	110	150	56.6
19	5	0.8	110	150	53.7	41	5	1.5	110	150	64.7
20	5	0.8	110	150	49.9	42	5	0.8	110	60	17.4
21	5	0.8	110	150	48.2	43	5	0.8	110	150	53
22	5	0.8	110	150	48.4	44	5	0.8	110	150	52.1

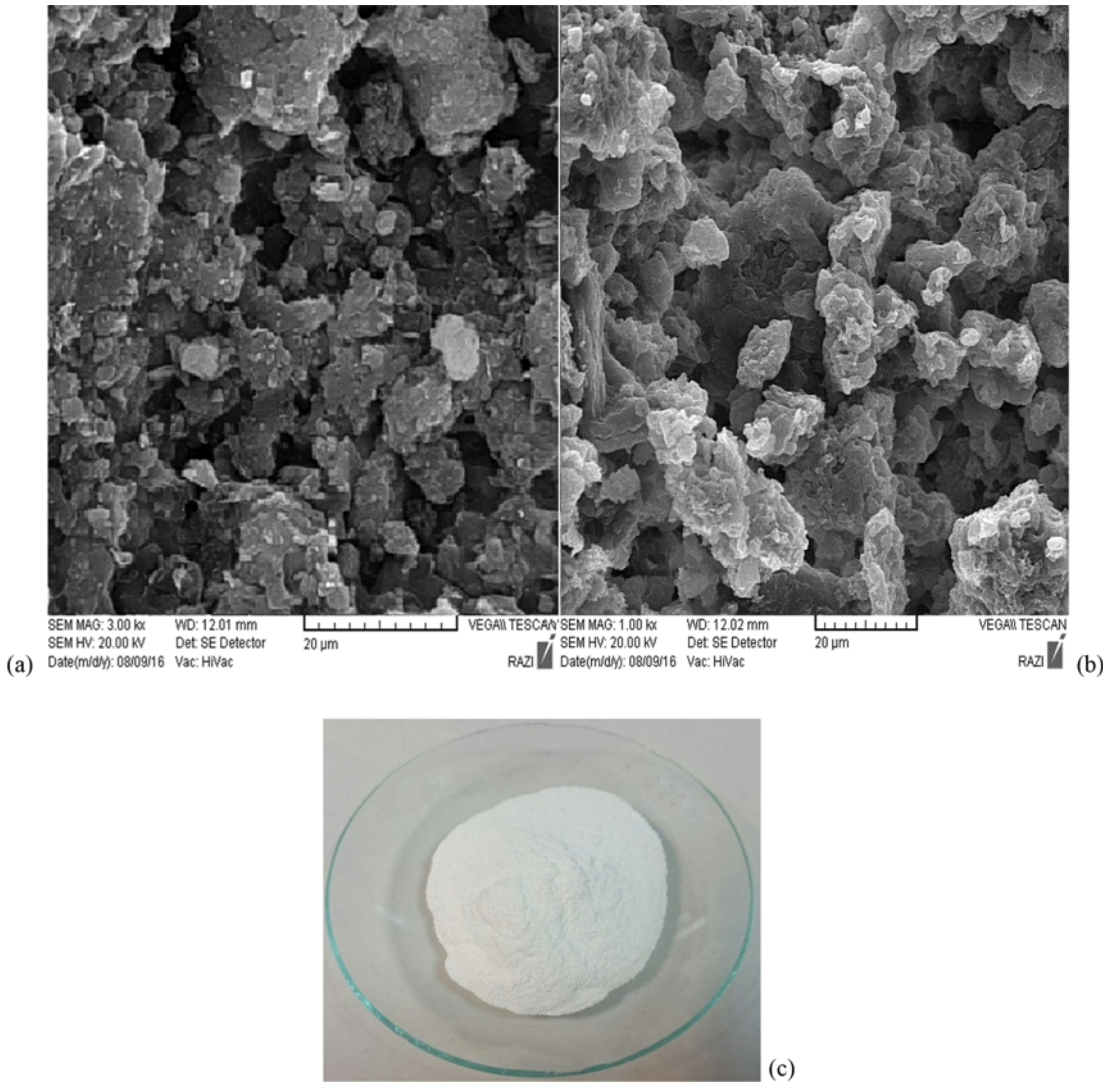

Fig. 3. SEM images of MBC: before (a) and after (b) As(V) removal, schematic of fabricated MBC (c).

where A_i is the dimensionless coded value of the ith independent variable, X_i is the uncoded value of the ith test variable, X_0 is the value of X_i at the center point, and ΔX is the step change value.

Experimental design of variables and the considered levels for As(V) adsorption are shown in Table 1. A total 44 runs were designed, consisting of 2×4=8 axial points, 2^4=16 design points and 20 center points. The details of the experiments are given in Table 2. The adsorption behavior of the system is explained by the following empirical second-order polynomial equation:

$$Y = b_0 + \Sigma_{i=1}^{k} b_i X_i + \Sigma_{i=1}^{k} b_{ii} X_i^2 + \Sigma_{i=1}^{k-1} \Sigma_{i=2}^{k} b_{ij} X_i X_j + \varepsilon \quad (4)$$

where, Y represents the dependent variable (arsenic removal efficiency), b_0 is a constant value, b_i, b_{ii}, and b_{ij} refer to the regression coefficient for linear, second order, and interactive effects, respectively, X_i, and X_j are the independent variables, denotes the error of the model [23].

The results were analyzed by applying the analysis of variance (ANOVA), coefficient of determination (R^2), and response plots. Experimental ranges and levels of the independent variables considered for As(V) adsorption are given in Table 1. The experimental design and statistical analysis of the data used "R" software (version 3.0.3: 2014-03-06).

RESULTS AND DISCUSSION

1. Characterization of Modified Bentonite Chitosan

1-1. Scanning Electron Microscopy (SEM)

The SEM image of the MBC before and after As(V) adsorption, depicted in Fig. 3, was used to study MBC surface morphology. Based on the figure, the synthesized adsorbent is suitable for arsenic removal from aqueous solution due to its porous structure, which can provide high surface area for good adsorption.

1-2. XRD Analysis

The XRD patterns of sodium bentonite (BNa), BNa-CTAB, chitosan, chitosan-oxalic acid and MBC are shown in Fig. 4. A typical diffraction peak of BNa is 5.75°, responding to a basal spacing of 1.52 nm. After intercalation with surfactant, the typical diffraction peak of bentonite moves to lower angle (4.412°), responding to a

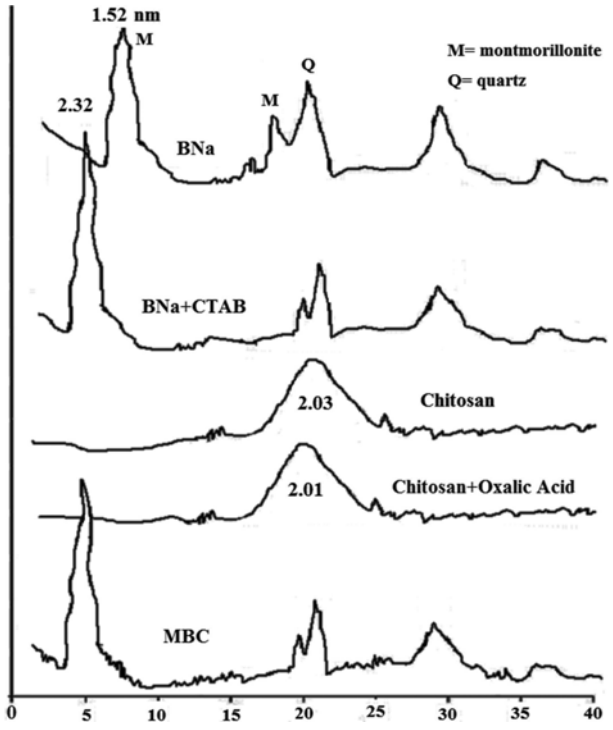

Fig. 4. XRD patterns of the samples.

basal spacing of 2.32 nm. The X-ray diffraction analysis of modified bentonite chitosan exhibits an increase in d-spacing compared to BNa, indicating the formation of intercalated structures. The predominant peaks were related to the montmorillonite (M) and quartz (Q). Thermal and chemical treatment changes the clay structure, decreasing the intensity of the typical peak of montmorillonite, inducing a possible distortion in octahedral and tetrahedral layer arrangement. The X-ray diffraction analysis of MBC exhibits an increase in d-spacing compared to BNa, indicating the formation of intercalated structures. The adsorption of As(V) on the surface of MBC was confirmed from the energy dispersive X ray (EDX) spectrum (Fig. 5) which shows the presence of arsenic with the other elemental constituents.

Table 3. Estimated parameters and their significance

Variable	Coefficient estimate	Std. error	T-value	P-value
Intercepts	53.22	0.78	67.80	2.2e-16
X_1	−19.20	1.41	−13.56	4.3e-14
X_2	27.44	1.41	19.37	2.2e-16
X_3	−12.36	1.38	−8.90	8.6e-10
X_4	19.99	1.41	14.11	1.5e-14
X_1X_2	−10.22	3.46	2.9475	0.006
X_2X_3	−13.17	3.46	−3.7978	0.0006
X_2X_4	19.37	3.46	5.5850	4.9e-06
X_1^2	−23.11	2.36	−9.7601	1.1e-10
X_2^2	−12.11	2.36	−5.1151	1.8e-5
X_4^2	−14.81	2.36	−6.2552	7.9e-07

2. RSM Approach for Optimization of As(V) Adsorption on MBC

As(V) removal was optimized by using response surface methodology (RSM). The removal percentage of As(V) depends on the individual and combinations of test variables, and the results show a significant variation for each combination. The relationships between response value and four independent variables could be markedly seen in contour and 3D surface plots in the following sections. The empirical relationship between As(V) removal (Y) and the four variables obtained by the application of RSM is given by the following quadratic model:

$$\text{Efficiency}_{As(V)} = 53.22 - 19.20X_1 + 27.44X_2 - 12.36X_3 + 19.99X_4 - 10.22X_1X_2$$

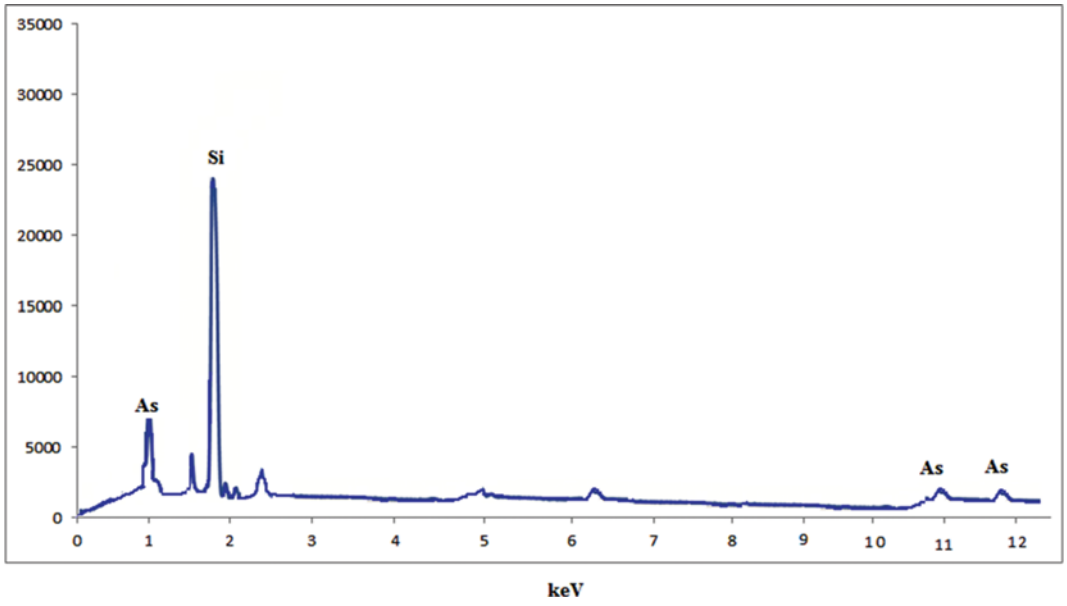

Fig. 5. Energy dispersive X ray spectrum of the adsorbed As(V) by MBC.

Table 4. Analysis of variance (ANOVA) of the response surface quadratic model for As(V) removal

Sources	Degrees of freedom	Sum of squares	Mean square	F-value	Prob>F
Second-order response	4	9999.7	2499.91	207.7	2.2e-16
Pure quadratic response	4	2231.9	557.96	46.3	3.4e-16
Residuals	29	349.0	12.03	-	-
Lack of fit	11	152.2	13.84	1.26	0.3173
Pure error	18	196.8	10.93	-	-

Notes: F-statistic: 76.67 on 14 and 29 DF, p-value: <2.2e-16, Multiple R^2: 0.973, Adjusted R^2: 0.961, Lack of fit: 0.3173

$$-13.17X_2X_3+19.37X_2X_4-23.11X_1^2-12.11X_2^2-14.81X_4^2$$

where X_1, X_2, X_3 and X_4 are solution pH, sorbent dosage, initial As(V) concentration and contact time, respectively.

Analysis of variance was used to analyze the significance and adequacy of the regression model. The results from the ANOVA for the quadratic equation are summarized in Table 3. The coefficient of variation and F-value tests were also performed for the evaluation of model goodness. The smaller the value of P and the larger the value of F, the more significant is the corresponding coefficient term [24,25]. For the adsorption of As(V) by MBC, the ANOVA results indicated that the F-value for the model was 207.7. As seen in Table 3, the most significant term of the regression model was the sorbent dosage (X_2) for the present application (T=19.37, P=2.2e-16). The positive coefficients for the model terms (X_2, X_4, and X_2X_4) indicated a favorable or synergistic effect on the As(V) removal percentage, while the negative coefficients for the model terms (X_1, X_3, X_1X_2, X_2X_3, X_1^2, X_2^2 and X_4^2) showed an unfavorable or antagonistic effect on the As(V) removal percentage. The determination coefficient (R^2) of the model was 0.973, indicating that prediction of As(V) removal efficiency by the quadratic model was excellent. Moreover, the value of lack of fit for the model was 0.3173 which implied that the lack of fit was significant. Table 3 shows that the linear coefficients (X_1, X_2, X_3 and X_4), cross product coefficient (X_1X_2, X_2X_3 and X_2X_4) and quadratic term (X_1^2, X_2^2 and X_4^2) significantly affected the As(V) removal efficiency by MBC (P< 0.05). The other model terms whose P-values were not significant

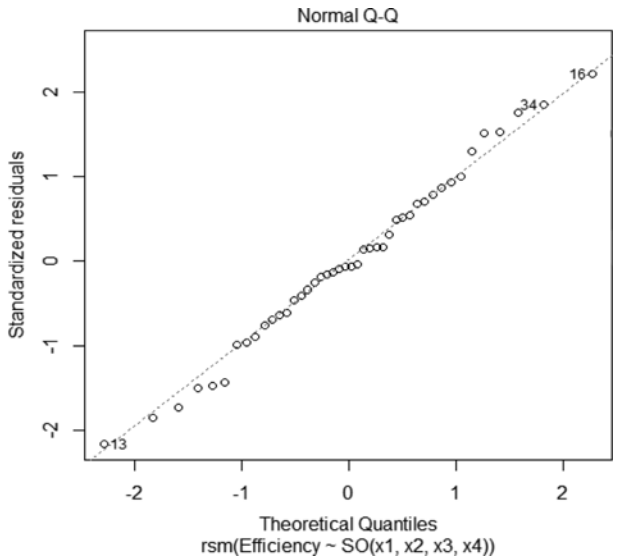

Fig. 6. Normal probability plot of residuals for As(V) removal.

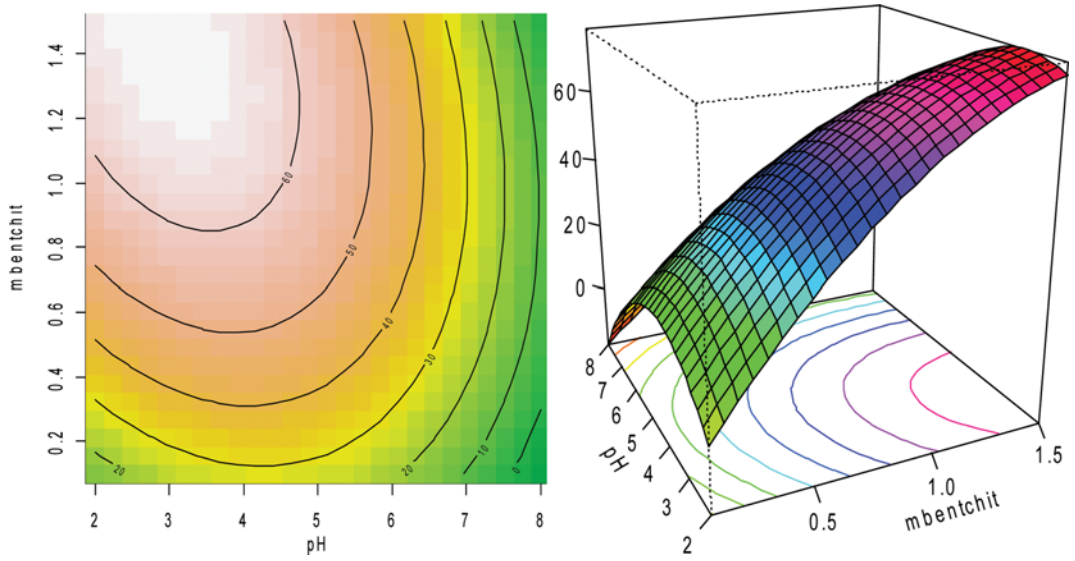

Fig. 7. The contour and 3D plots exhibiting the interactive effects between pH and sorbent dosage.

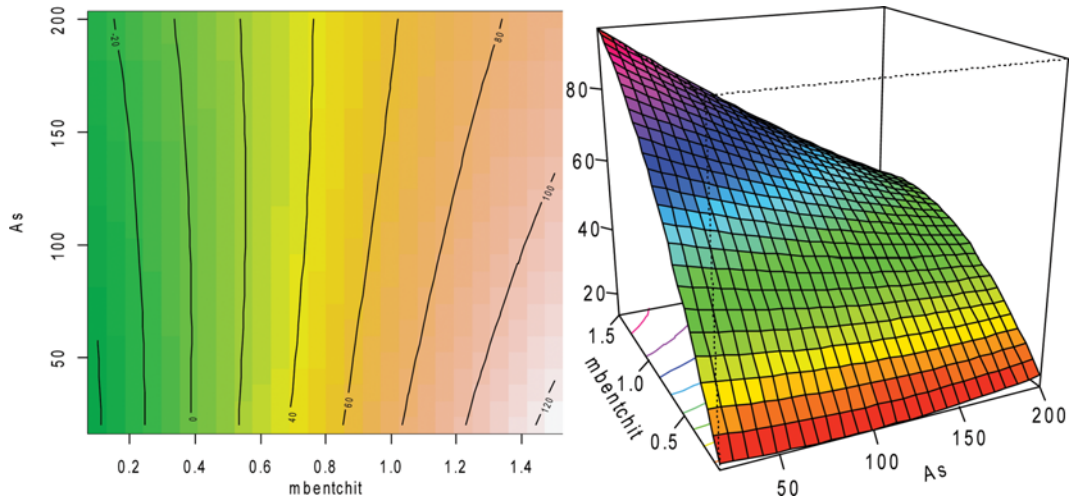

Fig. 8. Effect of sorbent dosage and arsenic ion concentration on % removal of As(V) by MBC.

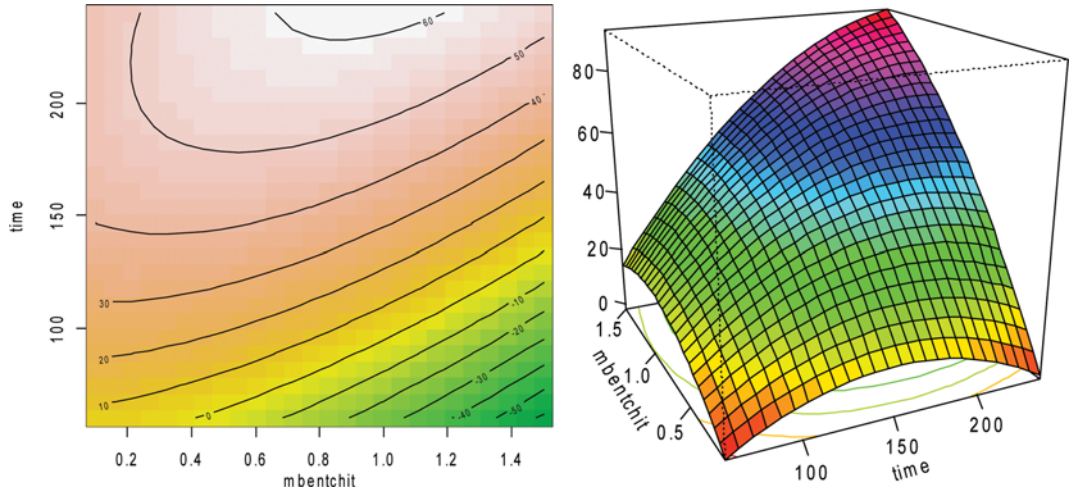

Fig. 9. The contour and 3D plots exhibiting the interactive effects between sorbent dosage and contact time.

(P>0.05) were removed from the table.

The experimental data accuracy was examined by performing a normal probability plot. Generally, the residuals in the plot should obey a straight line. Fig. 6 depicts the normal probability plot of residual values [26]. The above finding shows the accuracy and applicability of the central composite design (CCD) model for As(V) removal process optimization. The relationship between the independent and dependent variables was further elucidated by constructing contour plots.

3. Effect of pH and Sorbent Dosage

We studied the effect of pH on MBC adsorption percentage in the range of 2-8. The combined effect of pH and sorbent dosage on the uptake of As(V) by MBC is depicted as contour and 3D plots in Fig. 7. The plots provide a straightforward description of the effects of the independent variables on the dependent variable [25]. Under strong acidic environment (below pH 2), the chitosan undergoes dissolution and solidifies in alkaline media [27], which decreases the removal percentage. Fig. 7 clearly depicts that the sorption percentage of MBC for arsenic depends on the solution pH, increasing with a decrease in pH, and thus maximum adsorption occurred in the acidic range. The decrease in As(V) sorption was remarkable as the pH increased from 2 to 8. Moreover, the extent of As(V) adsorption on MBC is dependent on the stability and affinity of the arsenic species. Generally, the predominant As(V) species existing in the pH ranges are AsO_4^{3-} (pH>12), $HAsO_4^{2-}$ (pH=7-11), $H_2AsO_4^-$ (pH=2-7), and H_3AsO_4 (pH<2). Experimental data suggested that the predominant arsenic species adsorbed should be $H_2AsO_4^-$ [28]. The sharp reduction in arsenic removal might be explained as follows. In one respect, with further increasing pH value, a more negatively charged species of $HAsO_4^{2-}$ began to dominate in the solution. In the same time, the charge of binding sites on the surface of MBC became more negative, which considerably enhanced the repulsive force between the arsenic species and the binding sites. Therefore, the removal of As(V) was evidently depressed.

4. Effect of Sorbent Dosage and As(V) Ion Concentration

Combined effects of sorbent dosage and As(V) concentration on adsorption efficiency of arsenic by MBC are shown in Fig. 8.

The percentage removal increased as the sorbent dosage increased from 0.1 to 1.5 g (Table 2). At higher sorbent dosage, more binding sites become available for the uptake of As(V) onto MBC surface, which results in high removal efficiencies. From the results summarized in Table 2, a maximum removal of 93.7% was attained at dosage of 1.15 g MBC. Inversely, increasing the contaminant concentration involves a reduction in As(V) removal. Generally, higher sorbent dosage and lower arsenic concentration increased As(V) removal percentage.

5. Effect of Sorbent Dosage and Contact Time

The effect of sorbent dosage and contact time on the removal percentage of As(V) is depicted in contour and 3D plots in Fig. 9. The effect of contact time on adsorption of As(V) onto MBC was studied over a shaking time of 60-240 min using different sorbent dosages. We found that the removal of As(V) ions increased with increase in contact time up to a certain time (167 min) and afterwards a negligible change was observed. Increase in adsorption percentage with increase in contact time can be attributed to the fact that more time becomes available for arsenic ions to make an attractive complex with MBC.

6. Isotherm Studies

The adsorption isotherm is key to understanding the mechanism of the adsorption process. From several isotherm models available in the literature, three important isotherms were selected in the present study: the Langmuir, Freundlich, and Temkin [29]. The Langmuir isotherm assumes monolayer adsorption of contaminant onto adsorbent surface with a finite number of biding sites without any interaction between adsorbed ions [30]. The Langmuir, Freundlich and Temkin isotherms can be represented by the following equations:

$$\text{Langmuir} \quad Q_e = \frac{Q_{max} K_L C_e}{1 + K_L C_e} \tag{5}$$

$$\text{Freundlich} \quad Q_e = K_F C_e^{1/n} \tag{6}$$

$$\text{Temkin} \quad Q_e = B \ln A + B \ln C_e \tag{7}$$

For Langmuir and Freundlich, Q_e (mg/g) is the equilibrium As(V) ion concentration in the solid phase; Q_{max} (mg/g) is the maximum quantity of sorption; K_L (L/mg) is the Langmuir sorption equilibrium constant; C_e is the concentration of solute at equilibrium or after adsorption; K_F (mg/g) (L/mmol)$^{1/n}$ is the Freundlich constant representing the sorption capacity, n is the constant depicting the sorption intensity.

For Temkin isotherm: B=RT/b, b is the Temkin constant related to sorption heat (J/mol), A is the Temkin isotherm constant (L/g), R is the universal gas constant (8.314 J/mol/K), and T is temperature at 298 K [31].

The maximum adsorption capacity of As(V) by MBC was obtained from the isotherm study. Therefore, batch adsorption isotherm experiments were carried out at varying initial concentration under optimized conditions at pH around 3.7 and temperature of 25 °C at 150 rpm. The results demonstrated the best fit to the Langmuir isotherm model for As(V), indicating that the monolayer of As(V) ions covers along MBC surface. Accordingly, maximum adsorption capacity of MBC for As(V) was 122.23 mg/g. Parameters of adsorption isotherm for MBC are given in Table 5. Adsorption capacity of this work (122.23 mg/g) was much higher than those reported in Song et al. (6.5 mg/g) and Dultz et al. (9 mg/g) due to several physical and chemical modification of bentonite and chitosan [32,33].

Table 5. Isotherm parameters for adsorption of As(V) on MBC at 25 °C

Isotherm	Parameters	Values
Langmuir	Qmax (mg/g)	122.23
	K_L (L/mg)	0.77
	R^2	0.99
Freundlich	n	4.59
	K_F (mg/g) (L/mmol)$^{1/n}$	60.41
	R^2	0.93
Temkin	A	0.35
	B	20.60
	R^2	0.98

7. Kinetics of Adsorption

We used two kinetic models, pseudo-first-order and pseudo-second-order, to calculate the kinetic parameters [44]. The adsorption kinetic parameters were studied on the batch adsorption of 200 ppm of As(V) at pH 3.7. The contact time was varied from 0

Table 6. Maximum adsorption capacities for As(V) adsorption onto different adsorbents

Adsorbent	Adsorption capacity (mg/g)	References
	As(V)	
Polymeric Al/Fe modified montmorillonite	21.23	[34]
Goethite	0.58	[35]
FMCB	39.1	[36]
Chitosan	58	[37]
Iron coated chitosan	16.1	[38]
TICB	2.1	[39]
Zirconium-loaded adsorbent	149.8	[40]
Chitosan-coated ceramic alumina (CH-CA)	96.46	[41]
Chitosan-coated gangetic sand (CH-GS)	23	[42]
Glutaraldehyde cross-linked chitosan (GLU-CH)	270	[43]

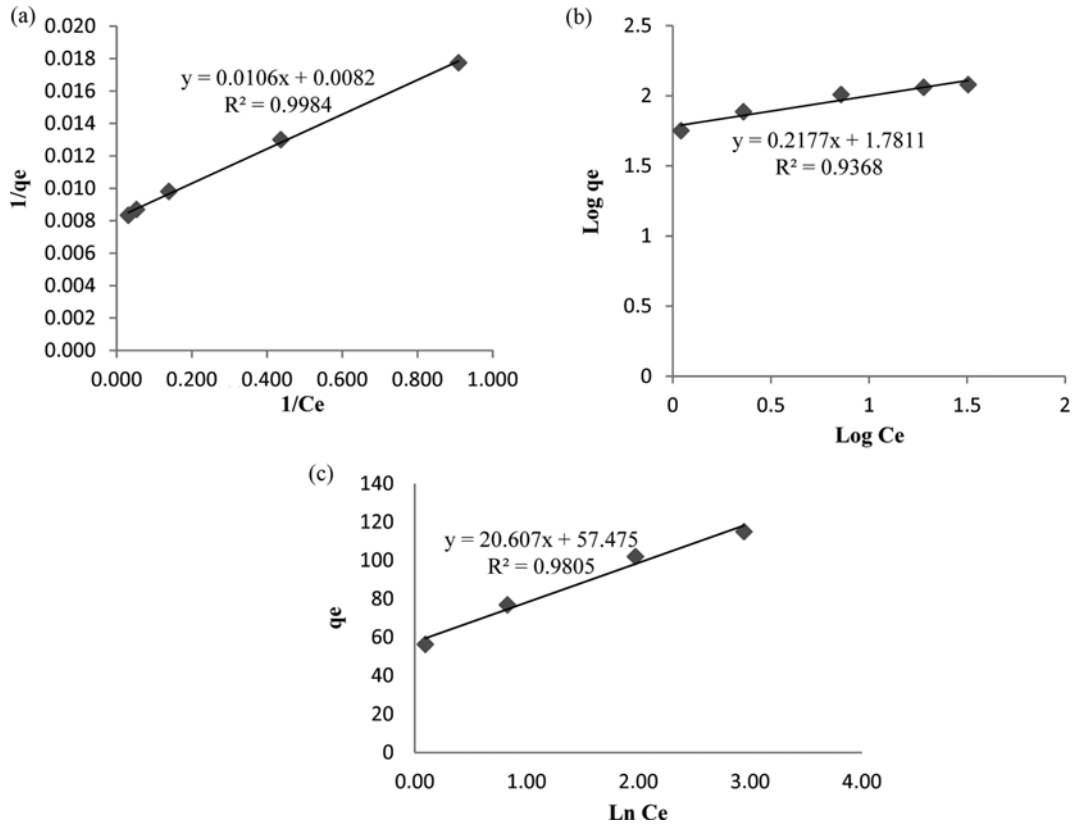

Fig. 10. Langmuir (a) Freundlich (b), and Temkin (c) plots for the adsorption of arsenic by MBC at 25 °C.

Table 7. Kinetic models fitted with the experimental data

Kinetic model	Formula	Plot
Pseudo first order	$\mathrm{Log}(q_e - q_t) = \log q_e - \frac{k_1}{2.303} \cdot t$	$\log(q_e - q_t)$ vs. t
Pseudo second order	$\frac{t}{q_t} = \frac{1}{k_2 q_e^2} + \frac{1}{q_e} \cdot t$	$\frac{t}{q_t}$ vs. t

Table 8. Constants obtained from kinetic models for As(V) adsorption onto MBC

C_0 [mg/L]	Pseudo-first order			Pseudo-second order		
	q_e (mg/g)	K_1 (min^{-1})	R^2	q_e (mg/g)	K_2 (min^{-1})	R^2
200	110.96	0.005	0.96	122.38	7.2E-05	0.99

to 3 h and the adsorption capacity of As(V) was monitored during the study. Each mixture was shaken at 150 rpm and 25 °C. The results of the regression analysis proved that As(V) adsorption on MBC was best described by the pseudo-second-order equation ($R^2 \approx 99\%$).

8. Thermodynamic Studies

The thermodynamic parameters, including free energy change (ΔG^o), enthalpy change (ΔH^o), and entropy change (ΔS^o), were used for feasibility study of the adsorption of As(V) on MBC. ΔG^o was calculated by use of the equation:

$$\Delta G^o = RT\mathrm{Ln}K_0$$

where K_0 is the thermodynamic equilibrium constant for the adsorption process, R is the universal gas constant, and T is the absolute temperature (K).

$$\mathrm{Ln}K_0 = \frac{\Delta S^o}{R} - \frac{\Delta H^o}{RT}$$

The values of ΔH^o and ΔS^o can be determined from the slope and intercept of the plot of $\mathrm{Ln}K_0$ versus 1/T [45]. The calculated values of the thermodynamic data ΔG^o, ΔH^o, and ΔS^o are summarized in Table 9. Based on the table, the decrease in ΔG^o with the increase of temperature indicated more favorable adsorption at higher temperature. The negative value of ΔS^o suggested the decreased randomness at the solid-liquid interface during the adsorption of As(V) onto MBC. In addition, the values of ΔH^o were found to be

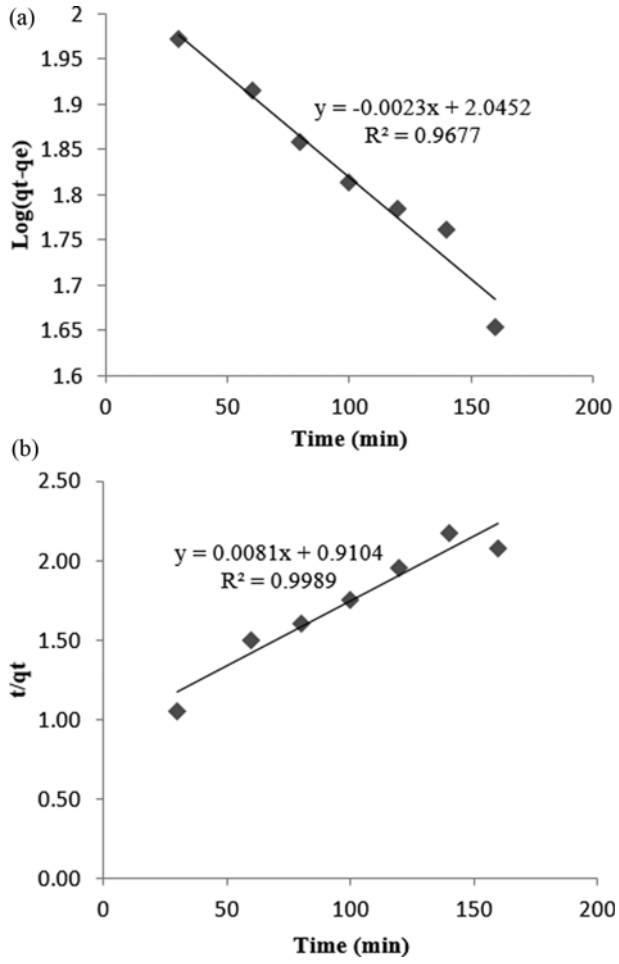

Fig. 11. Fitting the experimental data with (a) pseudo first order, and (b) pseudo second order kinetic models.

positive, which indicated the endothermic and physisorption nature of adsorption process [46].

9. Process Optimization and Confirmation

One of our main objectives was to determine the optimum process parameters for maximizing the removal of As(V) from aqueous solution. The Solver "Add-ins" was applied to determine the optimum condition for As(V) removal through the model equation predicted by RSM. Optimized values of pH, sorbent dosage, initial As(V) concentration and contact time were found as 3.7, 1.40 g/L 69 mg/L, and 167 min, respectively. To verify the validity of the predicted results by the model, several additional experiments were carried out in the experimental area of the CCD, and each experimental response was compared with the predicted one.

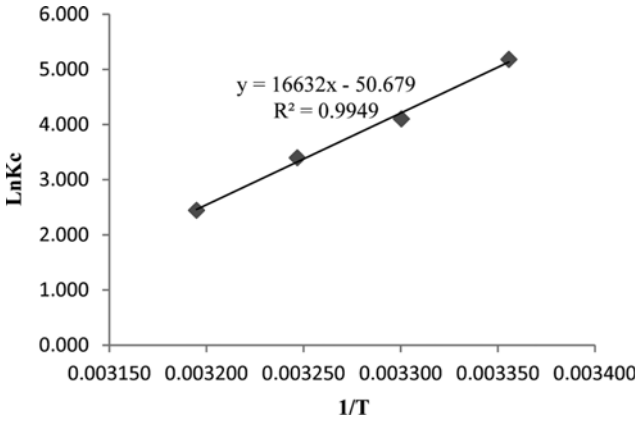

Fig. 12. Van't Hoff plot for estimation of thermodynamic parameters.

Comparison of the results with those predicted by Solver showed a good agreement.

CONCLUSION

We used bentonite and chitosan in modified forms (MBC) as two abundant and inexpensive materials for the removal of an important and toxic contaminant (arsenic) from aqueous solution. The experimental design of runs and the statistical analysis of the data involved using RSM in "R" software. The significant agreement between the model and experimental data was verified by ANOVA results. The results illustrated that a second-order polynomial regression model was capable of accurately explaining the obtained data. The model quality was tested through lack of fit, F and P values. Moreover, the MBC was characterized by SEM, XRD and EDX techniques. The SEM images clearly showed the removal of arsenic by MBC. The relationship between the independent and dependent variables was further elucidated by constructing contour plots. Optimized values of pH, sorbent dosage, initial As(V) concentration and contact time were 3.7, 1.40 g/L, 69 mg/L, and 167 min, respectively. The observed As(V) removal percentages under optimized conditions were consistent with the predicted findings from RSM. Overall, chitosan is much more expensive than bentonite; by the method of the present study, we improved the removal efficiency of the chitosan for arsenic by its combined use with bentonite. Moreover, the amount of applied chitosan was considerably reduced. The adsorption isotherms were also investigated. Among the isotherm models tested, the Langmuir isotherm model was the best fit for the obtained data, with a maximum adsorption capacity of 122.23 mg/g, thus indicating the monolayer adsorption behavior of the contaminant on MBC. The

Table 9. Thermodynamic parameters for adsorption of As(V) onto MBC

Adsorbent	Temperature (K)	ΔG^o (kJ·mol^{-1})	ΔH^o (kJ·mol^{-1})	ΔS^o (kJ·mol^{-1}·K^{-1})	R^2
MBC	298	−12.83	146.99	−350.60	0.99
	303	−10.33			
	308	−8.70			
	313	−6.36			

adsorption kinetics followed a pseudo-second-order kinetic model was involved in the adsorption process of As(V). Thermodynamic studies confirmed the spontaneous and endothermic character of adsorption process. The present work has shown that RSM provides a very reliable and accurate methodology for optimizing experiments for the removal of As(V) from aqueous solutions.

ACKNOWLEDGEMENT

The authors would like to thank Dr. Mehdi Zarrei for his useful advice for improving the text. We also wish to thank Mehdi Ghasemi, Zohreh Moeini, Hamed Biglari and Mansoureh Farhang for their excellent technical assistance, laboratory analysis and management support in Gonabad university of medical sciences. This research has been supported by the Tehran University of Medical Sciences, Institute for Environmental Research Code: 29990.

REFERENCES

1. A. Zehhaf, A. Benyoucef, C. Quijada, S. Taleb and E. Morallón, *IJEST*, **12**, 595 (2015).
2. C. Gerente, Y. Andres, G. Mckay and P. Le Cloirec, *Chem. Eng. J.*, **158**, 593 (2010).
3. A. Anjum, C. K. Seth and M. *Datta, Adsorp. Sci. Technol.*, **31**, 303 (2013).
4. Keshavarzi, F. Moore, M. Mosaferi and F. Rahmani, *Water. Qual. Expo. Health*, **3**, 135 (2011).
5. J. Qi, G. Zhang and H. Li, *Bioresour. Technol.*, **193**, 243 (2015).
6. P. Monvisade and P. Siriphannon, *Appl. Clay. Sci.*, **42**, 427 (2009).
7. W. H. Organization, *Guidelines for drinking-water quality: Recommendations*, World Health Organization (2004).
8. D. D. Gang, B. Deng and L. Lin, *J. Hazard. Mater.*, **182**, 156 (2010).
9. C. Septhum, S. Rattanaphani, J. Bremner and V. Rattanaphani, *J. Hazard. Mater.*, **148**, 185 (2007).
10. P. K. Dutta and J. Dutta, *Multifaceted development and application of biopolymers for biology*, Biomedicine and nanotechnology, Springer (2013).
11. R. Huang, B. Yang, Q. Liu and Y. Liu, *J. Appl. Polym. Sci.*, **131**, (2014).
12. M. W. Wan, I. G. Petrisor, H. T. Lai, D. Kim and T. F. Yen, *Carbohyd. Polym.*, **55**, 249 (2004).
13. C. M. Futalan, C. C. Kan, M. L. Dalida, K. J. Hsien, C. Pascua and M. W. Wan, *Carbohyd. Polym.*, **83**, 528 (2011).
14. N. Grisdanurak, S. Akewaranugulsiri, C. M. Futalan, W. C. Tsai, C. C. Kan, C. W. Hsu and M. W. Wan, *J. Appl. Polym. Sci.*, **125**, (2012).
15. M. C. Lu, M. L. Agripa, M. W. Wan and M. L. P. Dalida, *Desalin. Water. Treat.*, **52**, 873 (2014).
16. R. Huang, D. Zheng, B. Yang and B. Wang, *Energy Source. Part. A.*, **38**, 519 (2016).
17. Y. Xi, R. L. Frost, H. He, T. Kloprogge and T. Bostrom, *Langmuir*, **21**(19), 8675 (2005).
18. J. Guo, S. Chen, L. Liu, B. Li, P. Yang, L. Zhang and Y. Feng, *J. Colloid Interface Sci.*, **382**, 61 (2012).
19. K. Ba, L. He, H. Tang, J. Gao, S. Zhu, Y. Li and W. Sun, *KUI*, **63**, 253 (2014).
20. S. Hasan, A. Krishnaiah, T. K. Ghosh, D. S. Viswanath, V. M. Boddu and E. D. Smith, *Sep. Sci. Technol.*, **38**, 3775 (2003).
21. R. V. Lenth, *J. Stat. Soft*, **32**, 1 (2009).
22. S. Kalyani, A. Krishnaiah and V. M. Boddu, *Sep. Sci. Technol.*, **42**, 2767 (2007).
23. Q. Liu, B. Yang, L. Zhang and R. Huang, *Korean J. Chem. Eng.*, **32**, 1314 (2015).
24. H. Kalavathy, I. Regupathi, M. G. Pillai and L. R. Miranda, *Coll. Surf. B.*, **70**, 35 (2009).
25. Y. Liu, Y. Zheng and A. Wang, *Adsorp. Sci. Technol.*, **28**, 913 (2010).
26. G. Wang, S. Zhang, T. Li, X. Xu, Q. Zhong, Y. Chen, O. Deng and Y. Li, *RSC Adv.*, **5**, 58010 (2015).
27. D. W. Cho, B. H. Jeon, C. M. Chon, Y. Kim, F. W. Schwartz, E. S. Lee and H. Song, *Chem. Eng. J.*, **200**, 654 (2012).
28. A. Ramesh, H. Hasegawa, T. Maki and K. Ueda, *Sep. Purif. Technol.*, **56**, 90 (2007).
29. C. Umpuch and S. Sakaew, *Desalin. Water. Treat.*, **53**, 2962 (2015).
30. M. R. Samarghandi, M. Zarrabi, A. Amrane, M. N. Sepehr, M. Noroozi, S. Namdari and A. Zarei, *Desalin. Water. Treat.*, **40**, 137 (2012).
31. A. J. Jafari, B. Kakavandi, R. Rezaei Kalantary, H. Gharibi, A. Asadi, A. Azari, A. A. Babaei and A. Takdastan, *Korean J. Chem. Eng.*, **33**, 2878 (2016).
32. D. W. Cho, B. H. Jeon, C. M. Chon, Y. Kim, F. W. Schwartz, E. S. Lee and H. Song, *Chem. Eng. J.*, **200**, 654 (2012).
33. J. H. An and S. Dultz, *Clays Clay Miner.*, **56**, 549 (2008).
34. A. Ramesh, H. Hasegawa, T. Maki and K. Ueda, *Sep. Purif. Technol.*, **56**, 90 (2007).
35. B. J. Lafferty and R. H. Loeppert, *Environ. Sci. Technol.*, **39**, 2120 (2005).
36. J. Qi, G. Zhang and H. Li, *Bioresour. Technol.*, **193**, 243 (2015).
37. B. J. Mcafee, W. D. Gould, J. C. Nadeau and A. C. A. da Costa, *Sep. Sci. Technol.*, **36**, 3207 (2001).
38. A. Gupta, V. S. Chauhan and N. Sankararamakrishnan, *Water Res.*, **43**, 3862 (2009).
39. S. M. Miller and J. B. Zimmerman, *Water Res.*, **44**, 5722 (2010).
40. N. Seko, F. Basuki, M. Tamada and F. Yoshii, *React. Funct. Polym.*, **59**, 235 (2004).
41. V. M. Boddu, K. Abburi, J. L. Talbott, E. D. Smith and R. Haasch, *Water Res.*, **42**, 633 (2008).
42. L. Pontoni and M. Fabbricino, *Carhohyd. Res.*, **356**, 86 (2012).
43. P. Singh, J. Bajpai, A. K. Bajpai and R. B. Shrivastava, *Indian J. Chem. Technol.*, **18**, 403 (2011).
44. H. Khan, A. K. Khalil, A. Khan, K. Saeed and N. Ali, *Korean J. Chem. Eng.*, **33**, 2802 (2016).
45. M. Rani and S. Maken, *Korean J. Chem. Eng.*, **30**, 1636 (2013).
46. M. E. Argun, S. Dursun, C. Ozdemir and M. Karatas, *J. Hazard. Mater.*, **141**, 77 (2007).